ISABE 2009-1267

DESIGN OF A COUNTER ROTATING FAN - AN AIRCRAFT ENGINE TECHNOLOGY TO REDUCE NOISE AND CO_2-EMISSIONS

T. Lengyel, C. Voß, T. Schmidt, E. Nicke

German Aerospace Center DLR

Institute of Propulsion Technology
Linder Höhe, 51147 Cologne, Germany

Abstract

A model scaled (1:3) counter rotating fan was aerodynamically and mechanically designed using one of the newest design methods featuring a multiobjective automatic optimization method based on an Evolutionary Algorithm. This work was performed within the frame of the EU-project VITAL, which's objective is to contribute a significant part to the engine improvements towards the ACARE-goals, which are the noise reduction by 50 %, the NO_X reduction by 80 % and the CO_2 reduction by 50 %.

Three factors influence significantly the emission of noise, NO_x und CO2 in air-traffic: the engine, the airframe and the Air Traffic Management (ATM). The engine has an important contribution in achieving the ACARE-goals with a noise reduction by 10 dB, NO_X reduction by 60-80 % and the specific fuel consumption (SFC) reduction by 20 %.

The fan plays an important role for noise-emission and fuel consumption of the engine.

The increasing of the by-pass ratio (BPR) results in the reduction of the SFC and the reduction of the jet noise. The Direct Drive Turbo Fan and the Geared Turbo Fan are first steps in achieving noise reductions by increasing the by-pass ratio to 12 or even higher. This engine cycle concept requires maximal fan efficiency (Fig. 1). The counter-rotating fan concept promises a higher efficiency, further noise reduction by 6 dB at a BPR of 12, this is a total of 20 dB compared to the reference engine EIS2000. Therefore the development and improvement of the counter rotating concept was emphasized in one work package of the VITAL project.

In the context of the EU project VITAL, Snecma developed a counter rotating low-speed fan-concept for a high by-pass ratio engine. The detailed aerodynamic and mechanical design of the economic version was carried out by DLR and is subject of this paper. The economic version means in comparison with the basic design 20% reduction of blade numbers and a reduced axial gap was specified to decrease the engine weight, knowing that this could have unfavorable acoustic effects. The final design must have a good efficiency, sufficient stall margin and adequate acoustic performances for the given cycle parameter. SNECMA as the work package leader and developer of the concept defined the constraints and provided an initial geometry of the fan stage. The result of the design process is a counter-rotating fan stage with a high isentropic efficiency with sufficient stall margin. It should be emphasized that the maximal isentropic efficiency along the 100% speed line is exactly in the aerodynamically design point (ADP).

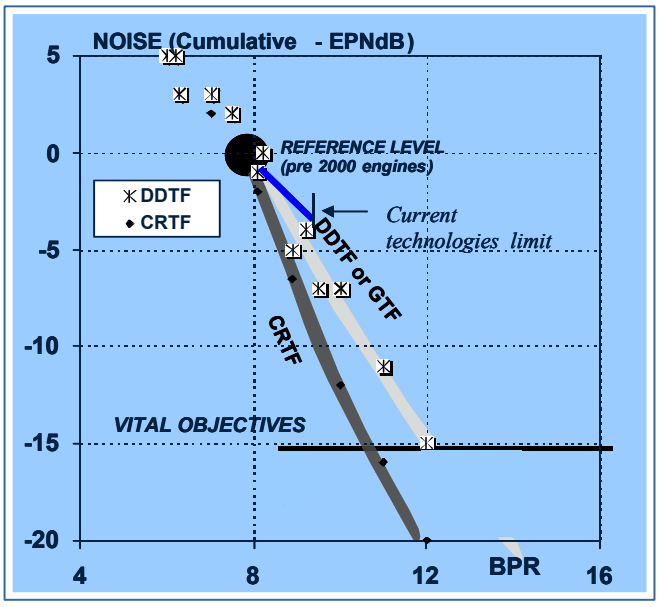

Fig.1: The promised noise reduction of the different fan technologies

Introduction

DLR was responsible for the aerodynamically and mechanical design, taking into account cycle definition, geometrical and other specifications of the fan stage and blade rows given by Snecma. The design process was divided into four phases:

Phase 0: analysis of the starting point and specifications; generation of an initial fan stage geometry.

Phase 1: aerodynamic optimization with mechanical constrains using the software package *AutoOpti* developed by

DLR (Institute of Propulsion Technology, Department Fan and Compressor). Two fitness functions were used: "Maximize the isentropic efficiencies at the aerodynamic design point (ADP) and at the working point for approach conditions". The 3rd calculated operating point is on the design speed line close to the stall margin. The multiobjective asynchronous algorithm was applied for generating more than 1000 calculated members in three working points. 128 free parameters were used allowing a wide range of blade shapes as well as hub and tip contour variations.

Phase 2: a selected geometry with high efficiency at the working line and with sufficient stall margin for the 100 % speed line was then analyzed in detail. A small number of parameter-studies were carried out to satisfy the aerodynamic goal including acceptable mechanical properties. Although the result of this study fulfills the specification, the second rotor showed clearly a potential for further improvement of the efficiency.

Phase 3: a second 3D optimization was carried out. The aerodynamic aspects were quite similar to Phase1, but here a real multi-physics optimization was applied: besides the aerodynamic fitness functions the Von-Mises-Stresses were calculated and utilized for a further fitness function.

As concluded in Phase2, the main focus was the improvement of the second rotor. Nevertheless for the first and second rotor a high number of free design parameter was taken into account to get a rotor pair which co-operates perfect on the whole working range. An increase of 1.5% in the efficiency at the ADP and about 12 % stall margin for 100 % rpm was achieved with the final geometry. The maximum efficiency is positioned mostly between the ADP and the stall point for the fan stages. The optimization provided a solution, where the maximum efficiency on the 100 % rpm is situated at the ADP, without dismissing the design specification of the 12 % stall margin.

Von-Mises-stresses of the blades and Campbell-Diagram calculations for both rotors were also included in the detailed mechanical analysis. Here a very close iteration between aerodynamic and mechanical design was realized.

Unsteady and flutter calculation were performed, the unsteady results were acoustically evaluated in terms of tonal sound emissions of the stage.

The optimized economic variant of the fan stage will be manufactured and tested in an anechoic test facility at CIAM in Moscow. The test results will feature the aerodynamic and acoustic performance of the new counter rotating fan configuration.

Nomenclature

CRTF	Counter Rotating Turbo Fan
BPR	Bypass ratio
ADP	Aerodynamic Design Point
SM	Stall margin
SFC	Specific Fuel Consumption
RPM	Rotational Speed [1/min] (also N)
β_{LE}	Leading edge angle
β_{TE}	Trailing edge angle
β_{ST}	Stagger angle
LT/TE	Leading Edge/Trailing Edge
Θ	Circumferential angle
Ma	Mach Number [-]
OP	Operating Point
p	Pressure [Pa]
T	Temperature [K]
r	Radius [m]
f	Frequency [Hz]

Subscripts

0	Nominal/Reference Conditions
abs	Quantity in Absolute Fram of Reference
rel	Quantity in Relative Frame of Reference
s	Static conditions
t	Total conditions

3-D DESIGN

Automatic Optimizer

The emergence of improved optimization algorithms and the performance enhancement of the newest super computing clusters nowadays enable the use of automatic optimization methodologies to perform complex multi-disciplinary and multi-objective optimization processes in turbomachinery design. Most of these methods are based on evolutionary algorithms (notation: EA) because of their potential to handle almost any kind of objectives: simple, very complex and even incomputable objectives coming from none converged simulations. [1][2][3][4]

In the past six years an MPI-parallelized multiobjective evolutionary algorithm with focus on turbomachinery applications, named *AutoOpti,* has been developed at the DLR Institute of Propulsion Technology. The following flowchart in Fig. 2 shows the basic structure of *AutoOpti*:

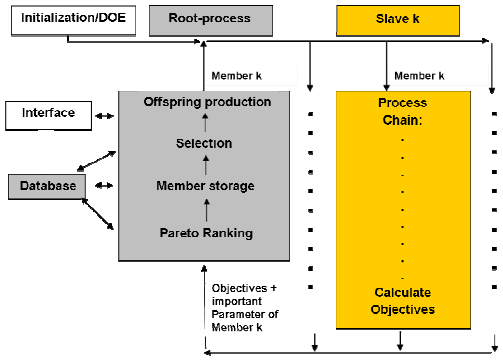

Fig.2: *AutoOpti* basic flow-chart

The optimization process is parallelized in an asynchronous manner using a master-slave communication.

The master-process mainly contains the optimization process (grey box on the left hand side of Fig. 2). In order to calculate the fitness values of a member, it hands the member over to a slave process (orange) and receives its fitness values and other important simulation results in return. The new evaluated member is stored in a database, and the Pareto rank (for a definition see Ref. [1]) is updated for all stored database members.

In the following selection step some members (notation: parents) are selected from the database for the production of a new offspring. The probability of selection is determined by the Pareto rank of each member. Several parents are recombined, using different operators like Mutation, Differential Evolution, or Crossover [1][3][4], to produce the offspring which is then send back to a corresponding slave-process.

The slave-processes (orange) are responsible for the faultless run of the considered process-chain. In general there are no mathematical constraints to that slave operator which maps the free optimization parameters to the fitness values (for example there is no need for this operator to be continuous or differentiable). Thus, this method has a large field of application without any constraints on the specific process-chain.

In aeromechanical compressor design the required process-chain is given by the flowchart of Fig. 3.

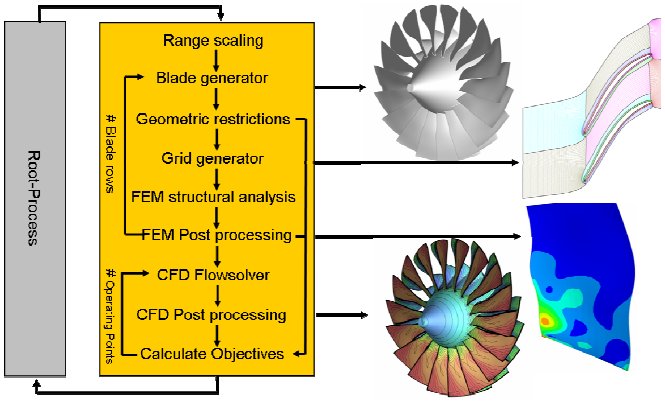

Fig. 3: Process-chain for compressor design

Key tools of the process-chain are the DLR-inhouse tools to generate flowpath, blades and grids, the DLR-inhouse CFD-solver for turbomachinery application TRACE (Ref. [7]), and the FEM-solver CalculiX (Ref. [8]).

In the following section, the most important special features of the program *AutoOpti* will be explained. These features distinguish *AutoOpti* from other optimization models and commercial tools. Most of them were developed in response to the enormous numerical effort of the process-chains in turbomachinery design (CFD and FEM for several operating points). Other features were implemented for a better handling and supervision of the optimization by the engineer.

Asynchronous Communication: *AutoOpti* is not population based. The parents of a new offspring are selected from the current database of all evaluated members rather than from the previous population. The benefit is an asynchronous communication between the root and the slave processes. In conventional evolutionary algorithms all slaves must wait until the slowest of them has finished before a new population can be generated. In contrast, the processor load in *AutoOpti* is almost 100% for all processes.

Restart and Constraint handling: Moreover, the database is essential for restart options and the setting up of metamodels (see next paragraph of this paper). For each member the set of free parameters, the objective values and all values of interest of a member (efficiency, mass flow, total pressure, total temperature, van-Mises stresses, …) are stored. This leads to a huge number of stored values (several hundred for typical turbomachinery applications). These values enable:

- A modification of the fitness functions at a restart of the optimization without any loss of information.
- Optimization observation by the engineer.
- Constraint handling: typical turbomachinery constraints can be monitored in consideration of these stored values. Unfulfilled **constraints** affect the Pareto rank and therefore the probability of selection of a member.

Interface: To make the optimization more controllable for the designer, an interface to the optimization process has been implemented (Fig.2). If during the optimization the root process detects any external design input in the interface (either by a human engineer or an external algorithm), these designs will displace the evolutionarily created offspring. Thus, the optimization process can learn from external information and engineer know-how.

Summarizing significant **advantages** of the EA-based program *AutoOpti* for aeromechanical compressor design:

- Multi-disciplinary optimization taken into account CFD and FEM results
- Potential to handle several objectives and constraints
- Chance to get over local Minima of fitness functions
- Controllable optimization process for the designer (interface)
- Restart-option without loosing information
- Parallelized asynchronously

The main **drawback** of basic-tool *AutoOpti* is the fact that EAs suffer from slow convergence because they use probabilistic recombination operators to control the step size and searching direction. It follows that - especially for expensive function evaluations – an EA typically requires a lot of CPU time. To damp that disadvantage of EA's, *AutoOpti* uses the acceleration potential of **Approximative Models:**

To accelerate *AutoOpti*, different approximative models are used. Since approximations are models of a simulation which is itself a model of reality, they are often called

metamodels (other notations: approximation, surrogate model, response surface). The basic idea of process acceleration using metamodels is quite easy to explain: The goal of using a surrogate model is to provide a functional relationship of acceptable fidelity to the "true" function with the added benefit of computational speed. The interaction between the original optimization and the metamodels is shown in Fig. 4.

While the original optimization is running (right hand side of figure 3), a second parallelized program is run for the training of metamodels and the optimization with these models (left hand side of Fig. 4) to find auspicious new members. Communication between these two programs occurs through the database (output of the original optimization and input for the metamodel training) and the interface (output of the metamodel optimization and input for the original optimization). The optimization on the metamodel in general strives for different goals than the original optimization and these metamodel objectives may change without interrupting the original CFD/FEM optimization.

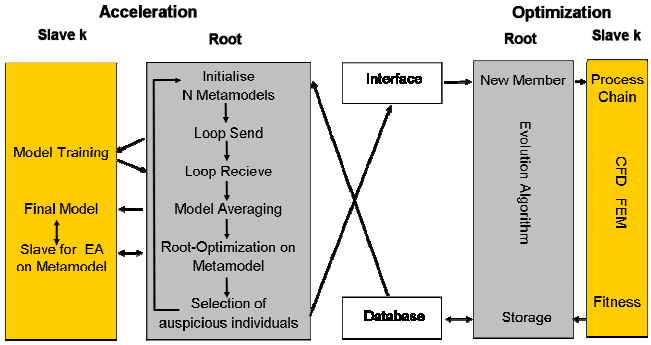

Fig.4: Metamodel acceleration

The details of how to build and exploit approximations effectively in high dimensional spaces, the selection of different infill sampling criteria like expected improvement, the improvement of the optimization schemes on the surrogate models, the averaging method of several models, etc., keep metamodel-based optimization a thriving research area. The metamodels implemented in *AutoOpti* are Kriging models and Bayesian trained Neural Networks [9]. They can be trained for any data set entry stored in the database. In addition these models can be trained binary to detect convergence vs. non-convergence behaviour.

Preparation of the optimization, the initial geometry

The application of the optimizer requires a complex preparation. An initial geometry has to be generated; it has to fulfill the specifications. The free variables have to be defined and limited with lower and upper limits according to the specifications. The objectives and the "so-called" region of interest have to be determined.

1. Generating the initial geometry

The sum of the number of the blades of both rotors was reduced by 20%. The axial length of the whole fan stage was also reduced to a specified value, which is consistent with realistic engine integration. Some other ratios concerning the chord length and the distance between the rotors, the limits of the aspect ratio, the minimal hub to tip ratio were also recommended. So based on these specification an initial geometry (flow path and blade geometry) for the optimization was created (Fig. 5).

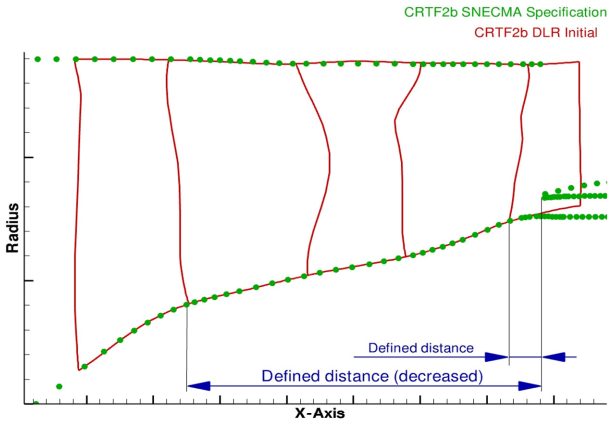

Fig.5: Initial flowpath

The designed blades had to be suitable for composite materials. To fulfill this objective a radial distribution of the blade thicknesses was specified by Snecma for example to take into account the bird impact on composite material blades. This includes not only the maximal thickness of the blade section but also thickness constrains at the leading edge and trailing edge (Fig. 6).

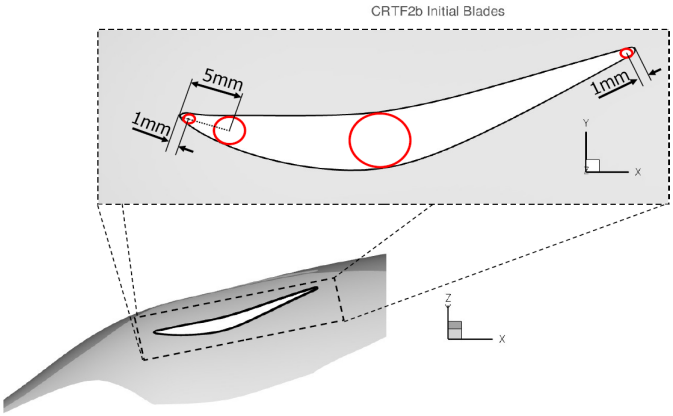

Fig.6: Thickness specification

2. Definition of the free variables and the limits of them

2.1 Flow path

The hub and tip-lines are described by splines in our design system. The splines are constructed by control points. 10 points of the hub-spline could be shifted with ±5 mm in radial direction and 11 points of the tip-spline could be shifted +3 mm and -5 mm also in radial direction (See the red dashed lines on the Fig. 7).

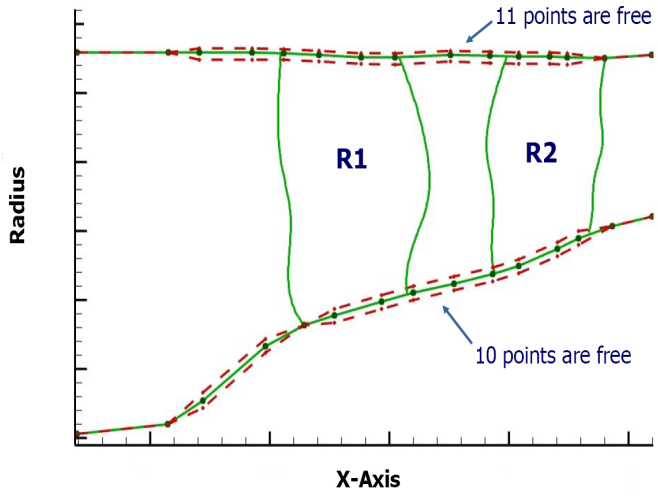

Fig. 7: Free parameter of the flow path

2.2 Blade parameters

The rotor blades are generated in our design system from 2D-profiles positioned on streamlines. The profiles are described by a set of parameters. For an optimization it is possible to set which parameters can be modified and in which limits. The free variables of this optimization were (Fig.8):

- Leading edge angle (β_{LE})
- Trailing edge angle (β_{TE})
- Stagger angle (β_{ST})
- X and Y coordinates of the construction points of the suction side spline (blue points in the Fig.8)

The pressure side was described by the definition of the thickness distribution. As stated above the thickness distribution was chosen for mechanical reasons and kept constant throughout the optimization.

Construction profiles were used in seven different blade heights to generate the 3D-geometry of the blade.

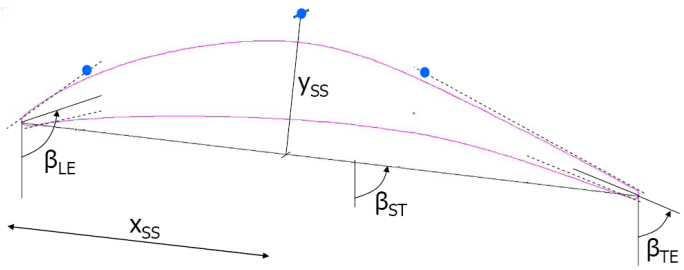

Fig. 8: Free parameter of the profile

The profiles can be shifted on the streamline in axial and circumferential direction before the stacking of the blade.

The position of leading edge and of the trailing edge in axial direction is prescribed by splines in the x-r coordinate plane. The x coordinates of the control points of the splines were free parameters within axial limits according to specifications for the maximal axial length of the stage and the minimal axial distance of the blades (Fig.9).

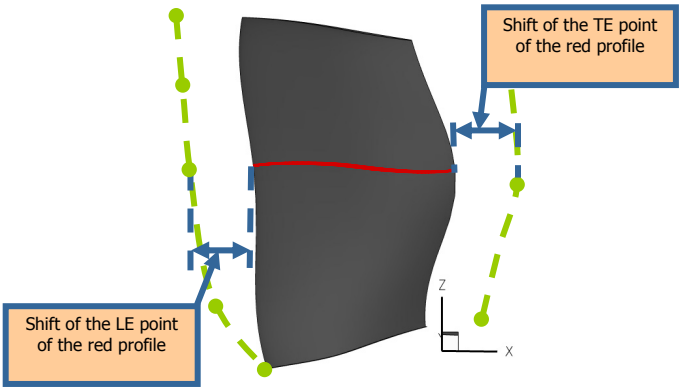

Fig. 9: Shift of the leading and trailing edges

The circumferential shift by a Θ angle has a strong influence on the mechanical balancing of the blades. Furthermore this parameter is very important for the aero-mechanical optimization. Therefore this angle is a free parameter for each profile (Fig. 10).

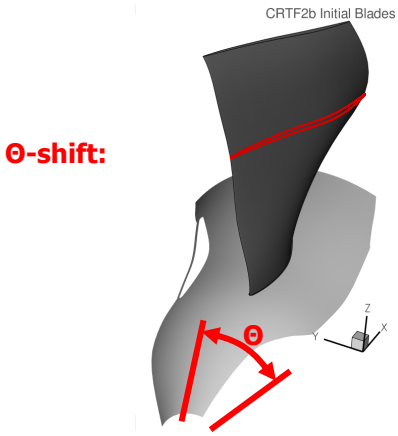

Fig. 10: Shift in the circumferential direction

128 free parameters were used in the first optimization and 82 in the second (See Fig.11).

Nr. of free variable		Opti1	Opti2
	Flowpath	21	0
R1	Theta-shift	6	6
	Leading edge	5	5
	Trailing edge	6	5
	Profiles	28	24
R2	Theta-shift	6	6
	Leading edge	7	5
	Trailing edge	7	3
	Profiles	42	28
		128	82

Fig. 11: Summary of the free parameters

In this paper only the final optimization (Opti2) will be presented in detail.

3. Determination of the objectives

The aerodynamically targets of the design of CRTF2b was a good efficiency at the Aerodynamically Design Point (ADP-100 % RPM) and at Approach on the working line. Previous optimizations showed that the efficiency at Approach correlated with the efficiency at ADP. Therefore the second optimization (Opti2) was focussed on the 100% speed line (Fig.12) and the efficiency at Approach was calculated afterwards.

Two objectives were taken into account at 100 % RPM:

- High efficiency at the working line
- At least 12 % stall margin

To achieve these objectives two operating points had to be calculated in the optimization:

1. ADP with the specified mass flow and pressure ratio. The target of this point was to obtain the maximal efficiency. (OP0)
2. A point near stall. Here the target was to increase the stall margin to at least 12 %. The CFD solver TRACE allows a simulation at specified mass flow. So a maximization of the total pressure ratio at this mass flow was used as the fitness function. The total pressure ratio had to be greater than a minimal value corresponding to the 12 % stall margin. (OP1)

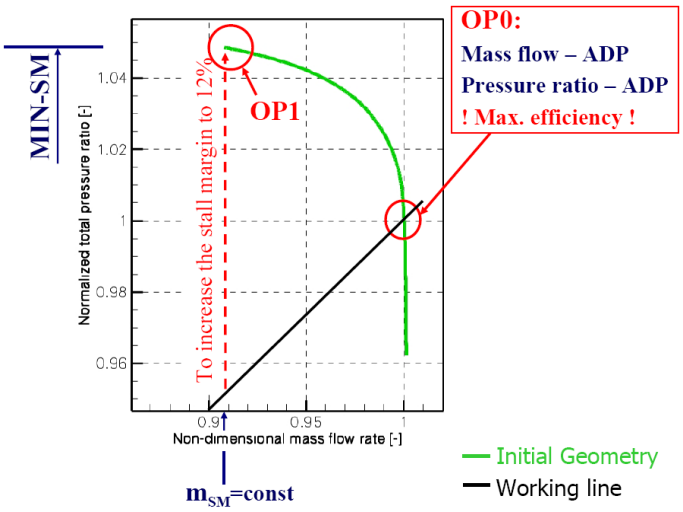

Figure 12: 100% performance line of the initial geometry

The mechanical targets of the blade design are defined in the specifications of Snecma. In the Project VITAL tests of the design concept on a test rig at CIAM in Moscow are planned. The test rotors will be manufactured as a blisk, the blades and the disc will be milled together from one raw part. This decision leads to simplified FEM-calculation. The blisks will be made of a special Ti-Al-Alloy. These material properties and characteristics provided the limitations for the statical and dynamical FEM-calculations.

In the automatic optimizer CalculiX is used to calculate the Von Mises stress distribution of a blade. Knowing the material properties a stress limitation was defined as a so-called “region of interest”. If the maximal stress – value of the FEM-result of a new geometry is outside the region of Interest (above the limitation), then this geometry gets a penalty in the pareto rang. The stress limitation in the FEM-calculations of the blades avoids generating unfeasible geometries. This is a huge advantage, considering both aerodynamically and mechanical properties simultaneously during the optimization.

The fitness functions and the region of interests are summarized in Figure 13.

	Fitness Function	Region of Interest	
OP0	Max. Efficiency!	Massflow rate: Totalpressure ratio: Exit swirl:	close to specified_i close to specified flow angle < 4°
OP1	Max. Pressure Ratio!	at selected Massflow	
R1+R2		Von Mises stress < Limit	

Fig. 13: The fitness functions and the region of interests

4. CFD mesh and CPU time

A mesh-sensitivity study and y-plus analysis was performed giving a final improved mesh, in which the cell size in the vicinity of the wall allows applying wall functions. [12]

A mesh with 550000 cells for the first rotor and 550000 cells for the second rotor, giving 1.100.000 cells for the whole stage was used.

Calculating one member took 6 hours in the two operating points with 6 CPUs, which means 36 CPU-hours per new calculated member. The optimization ran for 4 weeks with 60 nodes (120 CPUs). During this time 3400 geometries were generated, among these about 1600 geometries were calculated in 2 operating points.

5. Starting point and optimization goals

After the previous optimization a manual parameter-study based on the best geometry was realized. The target of this parameter study was to obtain a basic geometry for the final optimization which has an acceptable stress distribution and peak of Von Mises stress. This target is fulfilled after this study. This geometry was used as the initial geometry for the second optimization (black point in the Fig.14).

The main goal of the here discussed final optimization (Opti2) was the improvement of the isentropic efficiency at ADP especially in the second rotor and ensure the specifically SM and stress limits in parallel to avoid a further time consuming manual iteration process between mechanical and aero design.

Due to the project schedule the flow path was freezed and the number of free parameters reduced to 82.

Results of the final aeromechanical optimization

1. The data base

During the first 3 weeks the geometries, marked with blue points, were calculated. After a sufficient number of calculated members fulfilled the region of interest, the metamodell could be started. Through the metamodel an advanced region of interest could be set using a higher minimal efficiency and minimal total pressure ratio. The metamodel feeds the optimizer only those geometries with an expected efficiency and total pressure ratio above these minimal values. The new members, which are calculated in the optimizer after prediction by the metamodels, can be seen as green points in Fig.14. Most of the calculated values are near the predicted results.

In the best database the geometries are collected who's the pareto-rank equals 1 (red points in Fig.14). Therefore the final decision to choose the optimized geometry was the following simple process here: the member with the best efficiency in the best database is the optimized finally geometry.

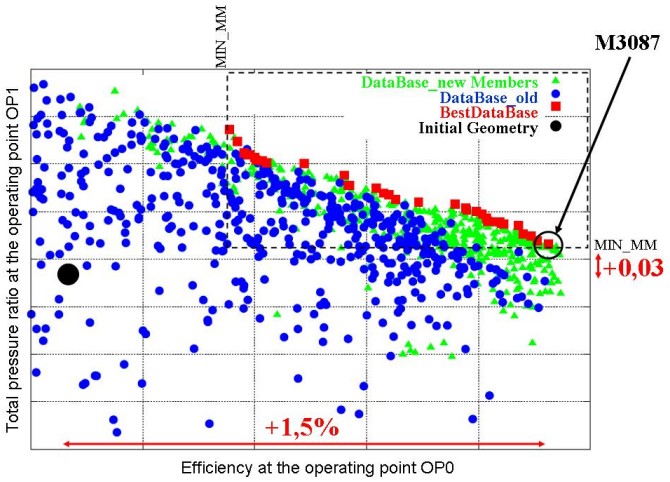

Fig.14: Pareto-front of the final optimization

2. Analysis of the selected geometry

The optimized geometry is compared with the initial geometry in Figure 15. A spectacular changing can be seen on the 3D view.

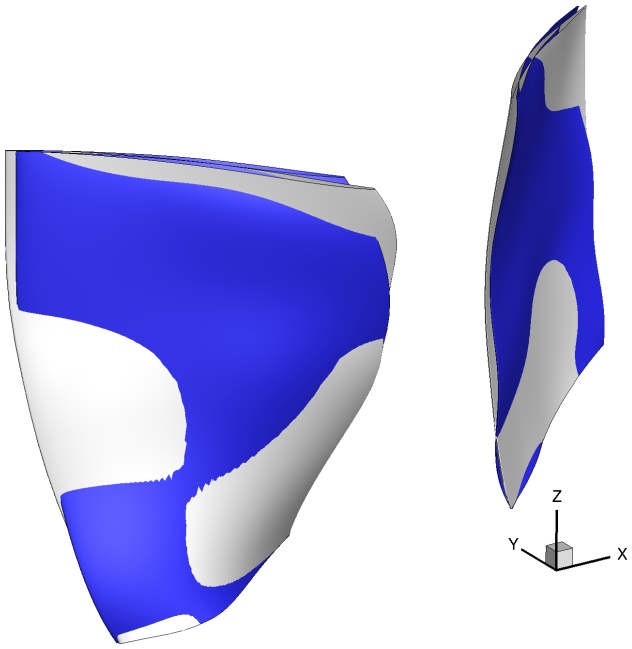

Fig. 15: The initial (blue) and the optimized geometry (grey)

With the changing of the free parameters to create the profiles on specified blade heights a significant changing of the isentropic Mach-number distribution was reached. In Fig.16 and 17 the Mach-number distribution along the profile on the middle section can be seen for the first and second rotor. The black lines show the result of the optimized geometry and the blue lines show the initial geometry.

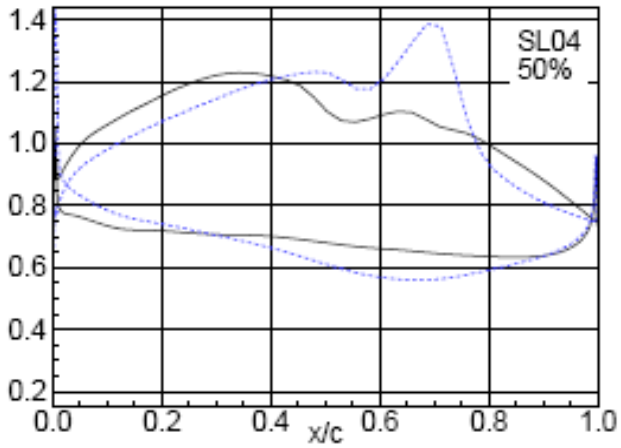

Fig. 16: Mach-number distribution along the profile on the middle-section of the R1 (The black lines show the result of the optimized geometry and the blue lines show the initial geometry.)

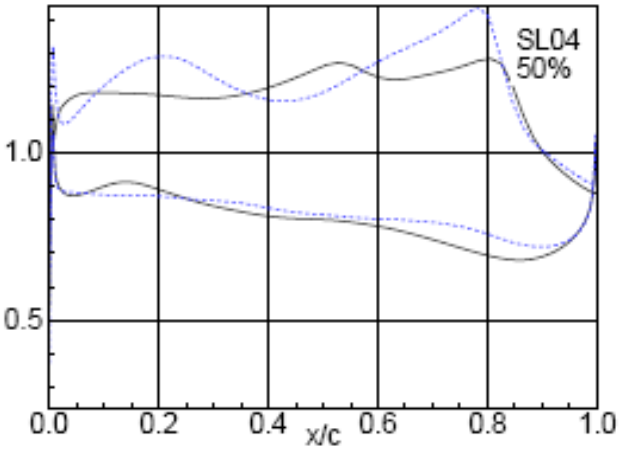

Fig. 17: Mach-number distribution along the profile on the middle-section of the R2 (The black lines show the result of the optimized geometry and the blue lines show the initial geometry.)

The Mach-number distribution in 2D on the middle-section can be seen in Fig. 18 and 19.Both visualization of the results shows a significant reduction of the pre-shock Mach-number. Before the optimization a pre-shock Mach-number of 1.4 can be seen along the first and second rotor. After the optimization this maximal value is about 1.2 for both rotors. This is valid not only for the mid-section but for the result over the whole blade height. This is the main reason for the efficiency improvement by 1.5%.

A comparison of the performance map of the initial and optimized geometry can be seen in Fig. 20. The operating point on the working line is the crossing point in the red square. One target of the design was to maximize the efficiency in this point. After the optimization 1.5% increase in efficiency in this point was realized. A huge advantage of this design can be observed on the 100%-performance map: the maximal efficiency is at the working point (ADP) on the design (100%) performance line and simultaneously 12 % stall margin was obtained. This is the most important result of this design task.

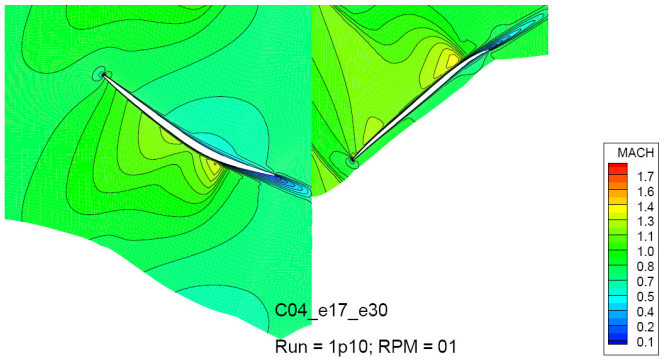

Fig. 18: Mach-number distribution of the initial geometry on the middle-section

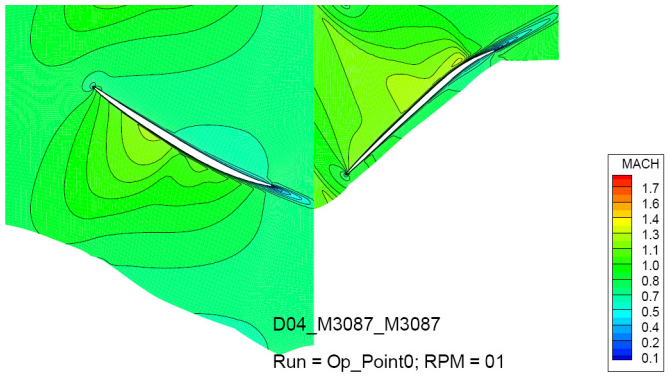

Fig. 19: Mach-number distribution of the optimized geometry on the middle-section

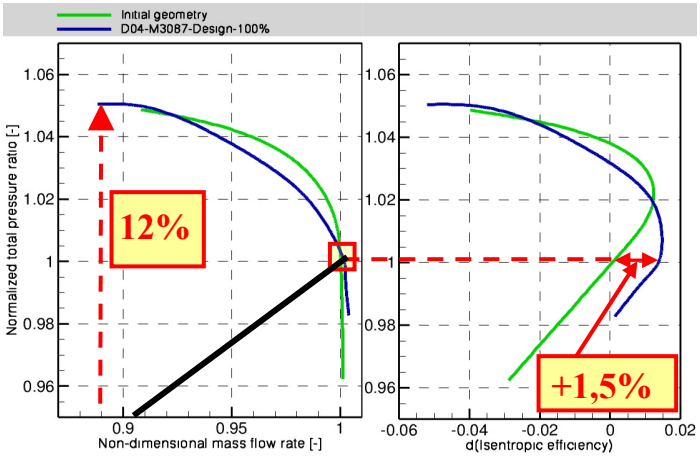

Fig. 20: 100% Performance map of the initial (green line) and optimized (blue line) geometry

The complete performance map of the optimized geometry was calculated and presented in Fig. 21. A comparison with the performance map of the CRTF1 is also presented on this figure. At the ADP of the CRTF2b is 3.5% increased efficiency observed compared to the same point of the

CRTF1. But these results are not completely comparable because of the different design-targets of the two different versions. Summarizing the results at different RPMs, a very good and uniform efficiency at the working line can be stated.

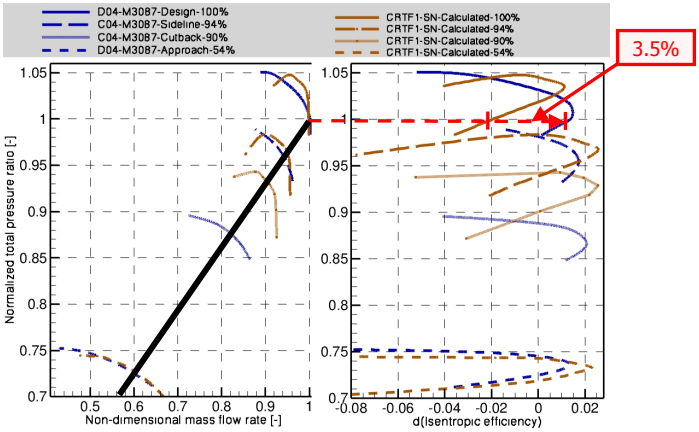

Fig. 21: Comparison of the performance map of the CRTF2b with the performance map of CRTF1

3. Detailed static FEM-calculations of the optimized geometry

The detailed structural analysis of the optimized geometry was realized with a high accuracy FEM-solver at DLR-Stuttgart. The Von Mises stress distribution on the first and second rotor is showed on the Fig. 22 and Fig.23.

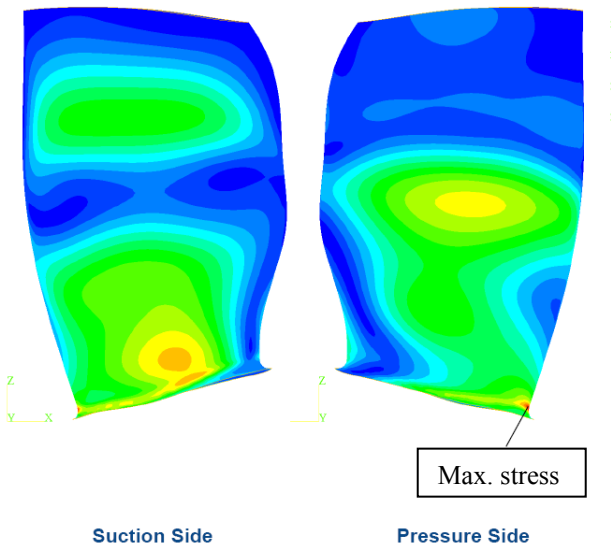

Fig. 22: The stress distribution on the first rotor (blue … low stresses, red … high stresses)

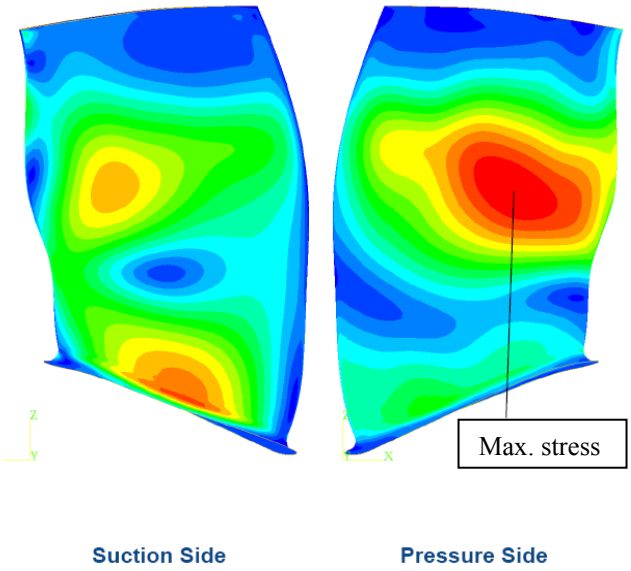

Fig. 23: The stress distribution on the second rotor (blue … low stresses, red … high stresses)

The maximal stress-values are under the defined limitation, so this geometry is suitable for the static requirements.

Conclusions and future works

A complete aerodynamic and mechanical optimization of the fan stage was carried out at the German Aerospace Center in Cologne (aerodynamic) and Stuttgart (mechanic). The multiobjective asynchronous algorithm was applied for generating more than 1000 in two working points calculated members. Two fitness functions were used: "Maximize the isentropic efficiencies at the aerodynamic design point (ADP) and the total pressure ratio near the stall". A Kriging-Model was used to accelerate the convergence of the optimization. Final Element structure analysis was also taken in account during the selection method.

The selected geometry with maximal efficiency at the working line and sufficient stall margin for the 100 % speed line was analyzed in detail. The performance map of the optimized geometry was compared with the performance map of the CRTF1 geometry. The design, sideline, cutback and approach operating lines were studied.

Advantages of this design compared with the CRTF1 geometry are the integration in the engine and the economical properties. This geometry is particularly interesting for the industry with regard to the reduced number of blades, axial length and a very good efficiency at ADP. Therefore a measurement of the acoustic properties, the unsteady behaviour and of the performance map is very important. The experimental examination is planned at the end of 2009 in Russia (Moskow) at CIAM on the same test bed where the CRTF1 geometry was measured. Acoustic measurement in an anechoic chamber will be realized. Kulite sensors will be

applied for the unsteady pressure measurement on the pressure side of the second rotor.

After the measurement the experimental results will be compared with the calculated results to validate the optimization.

References

[1] Voß, C., Aulich, M., Kaplan, B., Nicke, E., *Automated Multi-objective Optimisation in Axial Compressor Blade Design* , ASME Paper GT2006-90420

[2] Dorfner, C., Nicke, E., Voß, C., *Axis-Asymmetric Profiled Endwall Design Using Multi-objective Optimization Linked with 3D-RANS-Flow-Simulations*, ASME Paper GT2007-27268

[3] Voß, C., Becker. K., *Multi-objective optimization in axial compressor design using a linked CFD-solver*, ASME Paper GT2008-51131

[4] Rechenberg, I., *Evolutionsstrategie – Optimierung technischer Systeme nach Prinzipien der biologischen Evolution*, Stuttgart: Frommann-Holzboog, 1973

[5] Schwefel, H.P., *Numerical optimization of computer models*, Chichester: Wiley & Sons, 1981

[6] Giannakoglou, K. C., and Karakasis, M.K., 2006. *Hierarchical and Distributed Metamodel-Assisted Evolutionary Algorithms* , VKI Lecture Serieus 2006-03: Introduction to Optimization and Multidisciplinary Design

[7] Nürnberger, D., Ashcroft, G., Schnell, R., Kügeler, E., *Turbomaschinery Research Aerodynamics Computational Environment (TRACE) User´s Manual*, 2006

[8] Dhondt, G., *The finite element method for three-dimensional thermo mechanical applications*, ISBN 0-470-85752-8 Münich, Germany

[9] Siller, U., Voß, C., Nicke, E., *Automated Multidisciplinary Optimization of a Transonic Axial Compressor*, AIAA-2009-0863

[10] Kaplan B., *Design and Experiments of a Highly Efficient Low-Noise Fan Test Rig with Ultra-High Bypass Ratio*, PhD-Thesis University of Bochum and DLR-Report (Forschungsbericht) DLR-FB-2007-17, Institute of Propulsion Technology, 2007

[11] Kaplan, B., Nicke, Voss, C., *Design of a Highly Efficient Low-Noise Fan for Ultra-High Bypass Engines*, ASME-paper GT2006-90363, ASMT Turbo Expo 2006

[12] Weber, A., *3D Structured Grids for Multistage Turbomachinery Applications based on G3DMESH* Version 3.3, 2007

[13] Grieb, H., *Verdichter für Turbo-Flugtriebwerke*, ISBN 978-3-540-34373-8, 2009